Chapter 13

Integrated Gasification System for Power and Hydrogen Production

Lukman Adi Prananto and Muhammad Aziz

Additional information is available at the end of the chapter

http://dx.doi.org/10.5772/intechopen.71841

Abstract

The growth of economic and living standard leads to more electricity demand. Unfortunately, due to more limitation of power station area and electricity grid development, energy delivery issue is rising up; hence, new method of delivering the power by different energy carrier is necessary to investigate. Hydrogen has the promising potential as an energy carrier due to its high gravimetric energy density and cleanliness to the environment. For comfortable storage and transportation, hydrogen is covalently bonded to methylcyclohexane (MCH) and liquid organic hydrogen carrier (LOHC). In this chapter, novel integrated gasification systems for coproduction of electricity and MCH from low-rank coal and microalgae have been proposed. The total energy efficiency is improved by applying enhanced process integration (EPI) technology to minimize exergy losses throughout the integrated system. The integrated system for microalgae is capable to provide more than 60% of total energy efficiency, while the integrated system for low-rank coal delivers the total energy efficiency of 84%.

Keywords: H_2 production, low-rank coal, microalgae, enhanced process integration, chemical looping, hydrogenation, energy efficiency

1. Introduction

Owing to the impact of economic growth and living standard improvement, the requirement for electricity is always climbing up, and therefore more power generators have to be developed to supply the demand [1]. Also, due to limitation of potential area for the plant and the high investment cost of both power station and electrical grid, further approach to deliver the energy by different energy carriers is favorable to meet the energy demand [2]. By far, fossil fuels act as both primary energy sources and energy carriers for electricity generation. However, despite the proven and relatively highly energy-efficient technologies, the adoption of the fossil energy promotes high environmental impacts and drawback of sustainability [3].

Therefore, together with the concern of energy scarcity and environmental issue, further investigation to discover alternative energy carrier is required not only to complement the fossil energy but also for primary utilization by achieving highly efficient energy systems.

Several parameters need to be accomplished for the future energy carrier, including the simple production method, high energy density, and environmentally benign performance. To this, the hydrogen (H_2) has the promising potential as an energy carrier [4]. Under the ambient condition, H_2 owns high gravimetric energy density (120 MJ kg^{-1}), much higher than gasoline or natural gas, which leads to the extensive heat capacity [5]. However, against the potentials as the future energy carrier, H_2 has severe characteristics in the extremely low volumetric energy density (10.8 MJ m^{-3}) and boiling temperature ($-252.9°C$), which leads to the difficult transportation and storage methods [6]. Thus, instead of dispatching H_2 individually, some pretreatment to bond the H_2 into the more convenient form of carrier is very beneficial.

Currently, transportation and storage of H_2 are carried out by the various schemes, including liquefaction, compression, chemical and physical storages. An alternative solution for H_2 storage with high storage capacity and low-risk level can be approached by employing the liquid organic hydrogen carriers (LOHCs) [7]. Covalently bonding the H_2 through the hydrogenation process, the LOHCs have the capability to carry out 5–8 wt% of the H_2 content [8]. Due to the characteristics of high reversibility (hydrogenation and dehydrogenation processes) in the moderate temperature, low GHG emissions, simple storage, and comfortable transportation method by using vessel or pipeline, LOHCs own the potential for the application of long-distance and large-scale H_2 transportation [9]. Moreover, the infrastructure of LOHCs is relatively compatible with current method of fuel transportation, due to the liquid phase of the LOHCs in the room temperature and standard pressure condition [10].

The LOHCs cycle involves hydrogenation and dehydrogenation processes. In this process, the generated H_2 is exothermically reacted with the particular compounds in the catalytic hydrogenation [11]. Recently available LOHCs include cyclohexane-benzene, decalin-naphthalene, and toluene-methylcyclohexane (MCH) cycles [8]. In this chapter, toluene (C_7H_8)–MCH (C_7H_{14}) cycle is investigated as the LOHC cycle for the transportation and storage of H_2. Both toluene and MCH are low cost, stable compound, and high flexibility of transportation as the liquid phase is very reliable in the wide temperature range, which is favorable for long-distance transport and long-term storage. In addition to this understanding, Chiyoda Corporation, a well-established process engineering company in Japan, has testified the applicability of the toluene-MCH cycle in a relatively large-scale facility [12].

The investigation is emphasized on the effort of integrating the corresponding processes, including the drying, gasification, chemical looping, power generation, and the hydrogenation process to achieve optimum energy circulation based on enhanced process integration (EPI) to obtain the excellent energy efficiency of the total system. EPI is a technology to minimize thoroughly the heat loss of the system by applying the combination of exergy recovery and process integration [13]. With EPI, instead of the optimization of each process individually, the entire energy management of the system is observed to develop a high-efficient integrated plant with minimum waste of energy [14].

In this chapter, integrated gasification systems which hold capabilities for coproduction of electricity and MCH from different feedstocks are discussed. The investigation of the systems is emphasized on the overall design of the process scheme and evaluation of some operating parameters for system optimization. Low-rank coal [15] and microalgae [8] are chosen as the feedstocks for the integrated system due to the opposite characteristics from each feedstock. However, since both feedstocks are far away from the standard quality of fuel due to high moisture content, a pretreatment stage, including the drying process is discussed also in this chapter. To obtain a high overall efficiency of the integrated system, EPI is applied to implement the optimum benefits of heat energy and reduce the exergy destruction.

2. Enhanced process integration technology

The theory of EPI has been introduced and applied to several raw materials, including algae [16], coal [17, 18], biomass wastes [19, 20], and black liquor [21]. EPI is established from two core technologies such as the process integration and the exergy recovery. The latter relates to the concept to circulate the heat throughout a single process. By applying the EPI, overall exergy loss throughout the integrated system can be reduced as the total energy efficiency of the system is improved.

Figure 1 illustrates the principle of heat circulation employed in the integrated system, including an example of the application of the term of exergy elevation of the process stream. Here, the dotted and solid lines represent the cold and hot streams, respectively.

In contrast to conventional process integration technology, the intensification of the process regarding energy efficiency is carried out in EPI through heat circulation to minimize the exergy losses in each process module before performing the overall process integration. Hence, the energy/heat associated with the process is recovered efficiently by employing heat circulation that promotes exergy recovery.

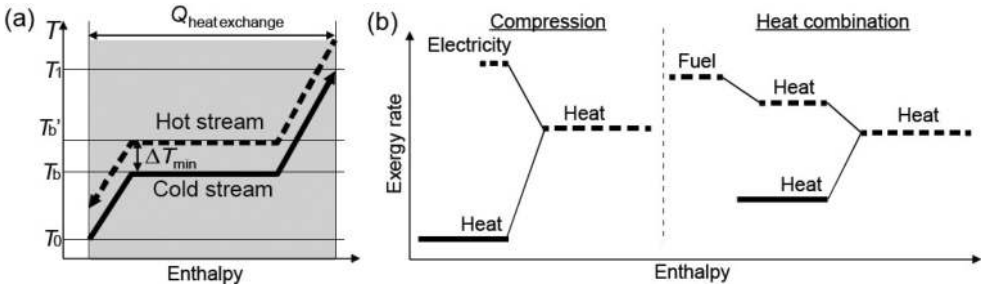

Figure 1. Basic heat circulation principle: (a) exergy elevation and heat coupling and (b) two examples of this method applied for stream exergy elevation: Compression and heat combination.

3. Power and H_2 production from various Feedstocks

3.1. Integrated systems from low-rank coal by syngas chemical looping

3.1.1. The characteristics of low-rank coal as energy source

Based on the current status of H_2 production, fossil fuel occupies dominant portion as the primary substance with more than 90% share [22]. In terms of sustainability, fossil fuel has a drawback in the issue of energy reserve. Hence, fossil fuel with abundant reserves is favorable for this system. One of the fossil fuel fit with this condition is low-rank coal (LRC). Besides the long-term reserves, LRC exhibits other advantages, including high concentration of volatiles, high reactivity, low sulfur content, and relatively low mining costs [23]. However, due to high inherent moisture content and readsorption behavior of the humidity, the drying of LRC is very challenging due to the energy intensive process [24]. Thus, an investigation based on EPI technology to effectively manage the heat circulation is carried out to develop an integrated system which can accommodate least expensive LRC for large-scale MCH production with optimum energy efficiency [25].

Another issue for the utilization of LRC is the large amounts of CO_2 emission, in which the plant has to be coupled with the CO_2 separation (capture) and sequestration facility. For the CO_2 capture, several technologies are available, including membrane, algae-based uptake, cryogenic, and chemical looping [26]. The latter is considered as the most potential method for the sequestration of CO_2 due to high capability of CO_2 capturing and high conversion efficiency.

Some investigations have been carried out to study the production of H_2 from coal. An integrated system consisting of hydrogasification, electrolysis, and electricity generation has been carried out by Minutillo and Perna [27] to produce synthetic natural gas. However, as the conventional process integration was adopted to develop the proposed system, the result of their study obtained relatively low energy efficiency due to significant losses of exergy. Another integrated system consisting of shell-type gasification, chemical looping, and electricity generation has been carried out by Xiang et al. In their proposed system [28], overall heat circulation was excluded, as the system adopted the pinch technology for heat recovery. Therefore, the system exhibits low energy efficiency. Moreover, Cleeton et al. carried out an integrated system with the combination of chemical looping and steam-coal gasification [29]. After the parameter evaluation, the delivered system showed energy efficiency up to 58%. However, if the effort of exergy optimization was applied, the energy efficiency of the system can be improved significantly.

3.1.2. Integrated system development

The schematic flow of energy and material of the integrated system is shown in **Figure 2**. Here, the dotted and solid lines represent electricity and material/heat flows, respectively. At the beginning of the process, the moisture content of raw LRC particles is extracted by the drying module. The product of this module is the high calorific value of LRC as the result of low moisture content. Next, the dried LRC particles are converted to syngas by the gasification module. The produced syngas is thus fed to the chemical looping module to generate H_2, CO_2,

http://dx.doi.org/10.5772/intechopen.71841

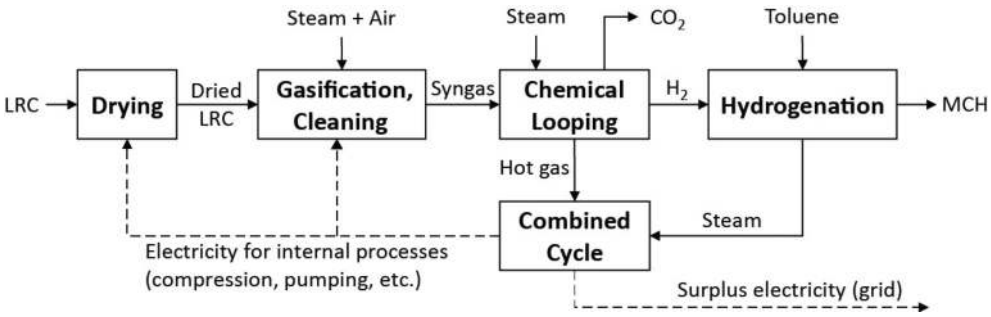

Figure 2. Schematic of material and energy flows in the integrated system.

and thermal energy for the power generation. The by-product of CO_2 generated in the chemical looping is sequestered to keep the clean energy of the integrated system, while the desired products of chemical looping are discharged to the combined cycle module and the hydrogenation module for the generation of electricity and MCH, respectively. The MCH is prepared in the liquid phase. Hence, the compound can be easily transported to the specified place. The generated electricity from the combined cycle is partially consumed for the house load operation for the internal processes, but the remainder can be sold to utilities via a connection to a power grid.

3.1.3. Analysis of integrated system

3.1.3.1. Drying and gasification

The drying process is carried out to meet the target of the moisture content of the LRC particle so that the calorific value is increasing and the high gasification temperature can be achieved. In the drying process, equilibrium moisture content significantly affects the immediate environment because the particle of LRC will reach a water concentration equal to the ambient environment. Hence, the temperature, pressure, and relative humidity of the environment, as well as the partial vapor pressure, determine the moisture content. Among any methods used for high moisture content drying process, the superheated steam exhibits numerous advantages, including the energy efficiency, high capacity, and has been widely investigated for drying scheme [30]. Thus, by employing the superheated steam as the drying method, the drying and gasification modules were developed, as shown in **Figure 3**. The relationship between the relative vapor pressure, p/p_o, and the equilibrium moisture content, M, can be approximated by Eq. (1) [31].

$$\frac{p}{p_o} = 1 - exp\left[-2.53(T_b - 273)^{0.47}\left(\frac{M}{(100 - M)}\right)^{1.58}\right] \quad (1)$$

Initially, the discharged heat produced in the chemical looping module and the high energy compressed steam is employed to preheat the high moisture content LRC particles (D1) in HX1 and HX2, respectively. Subsequently, the preheated LRC particles undergo drying process to omit the water content inside the particles. The type of dryer applied in this system is the

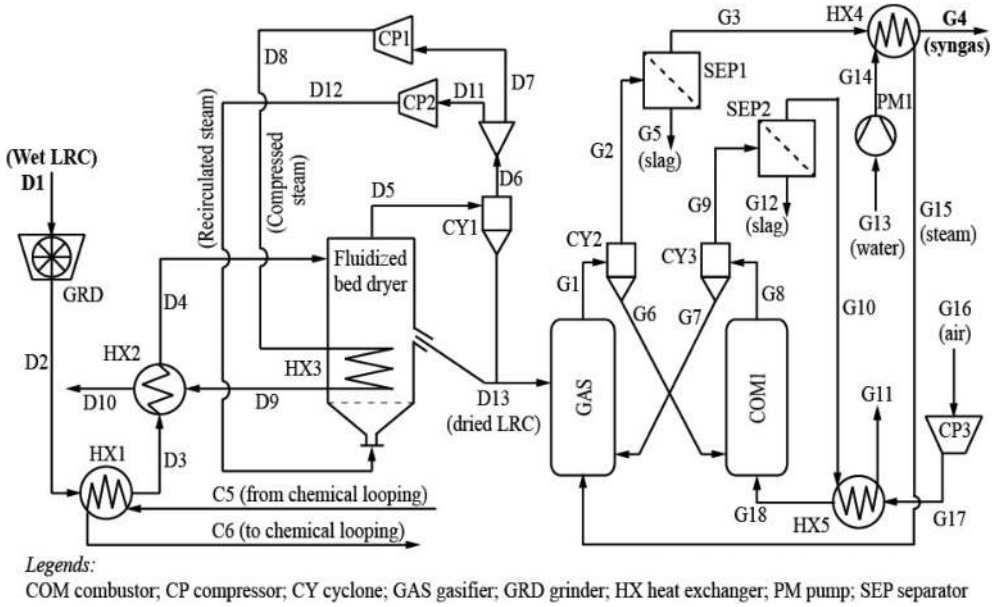

Figure 3. Schematic of drying and gasification modules.

fluidized bed owing to the benefit in the uniform temperature distribution and heat transfers, an extensive area of the contact surface, and proper particle mixing [32]. The immersed heat exchanger (HX3) is furnished inside the fluidized-bed dryer for the superheated steam process.

The next step is the gasification process, which produces combustible gases, including H_2, CO, and CH_4. Series of reactions are involved in this process, including the water-gas shift, Boudouard, and oxidation, as well as methanation. Due to the necessity of high gasification temperatures, dry-feeding gasification is employed in the system instead of slurry-feeding gasification [33]. Here, a dual-circulating fluidized bed (gasifier and combustor) is furnished to achieve higher carbon conversion efficiency and conversion rate [34].

After the gasification, both of the raw syngas and flue gas are fed into SEP1 and SEP2 for removal of ash and slag by the ceramic particulate removal which exhibits high efficiency under high-temperature conditions [35]. **Table 1** summarizes the conditions assumed for LRC drying and gasification study.

The effect of steam-to-fuel ratio during gasification is evaluated to define the optimum combination of steam and fuel. Two different steam-to-fuel ratios (0.9 and 1.4) are investigated to confirm the optimum ratio for the performance of the chemical looping system. **Table 2** shows the composition of the syngas resulting from different steam-to-fuel ratios.

3.1.3.2. Chemical looping and combined cycle

Among any methods, direct chemical looping and syngas chemical looping are the typical methods for the chemical looping. However, due to the utilization of the metal oxide for

Component	Value	Note
Drying conditions		
Coal flow rate (Mg h^{-1})	100	At moisture content of 18 wt% wb
Initial moisture content (wt% wb)	60	
Target moisture content (wt% wb)	18	
Fluidization velocity $U_{dry}/U_{mf,dry}$	1, 2, 3, 4	
Mean particle diameter (mm)	2.0	
Bulk density (kg m^{-3})	900	
Heating value (MJ kg^{-1} HHV)	19.33	
LRC ultimate analysis		
C (wt% db)	65.53	
H (wt% db)	3.75	
N (wt% db)	0.84	
O (wt% db)	25.22	
S (wt% db)	0.38	
Cl (wt% db)	0.05	
Ash (wt% db)	4.23	
Gasification conditions		
Combustion temperature (K)	1173	
Gasification temperature (K)	1123	
Steam-to-fuel ratio	0.9; 1.4	
LRC mean particle diameter (mm)	2.0	
Bed material	Olivine	
Mean bed material diameter (mm)	0.37	

Table 1. LRC drying and gasification conditions.

Produced syngas	Steam-to-fuel ratio	
	0.9	**1.4**
H_2 (Nm^3 kg-$fuel^{-1}$ daf)	0.820	0.762
CH_4 (Nm^3 kg-$fuel^{-1}$ daf)	0.063	0.066
CO (Nm^3 kg-$fuel^{-1}$ daf)	0.486	0.415
CO_2 (Nm^3 kg-$fuel^{-1}$ daf)	0.255	0.270
Steam content in produced gas (vol%)	19.1	28.7

Table 2. Composition of syngas generated using a dual-circulating fluidized bed with varying steam-to-fuel ratios.

oxygen carrier in the system, the syngas chemical looping is employed due to the beneficial in the solids handling and energy efficiency. The oxygen carrier exhibits no direct contact between atmospheric oxygen and the fuel during the combustion process; hence, the high-purity CO_2 can be immediately separated without any further handling, which thus promotes an efficient and clean energy conversion. Thus, due to the excellent mechanical properties, large capacity content of oxygen carrier, and the high conversion of syngas and steam, the iron-based materials are applied as the recirculated oxygen carriers [36].

Figure 4 represents a process flow diagram for the chemical looping and combined cycle modules. The chemical looping module is developed from three connected reactors: reducer (RED),

oxidizer (OXD), and combustor (COM2). In the reducer and oxidizer, a counter current moving bed reactor is employed, while an entrained fluidized bed is furnished for the combustor.

In the RED, the compressed syngas is fed as the fluidizing gas. After leaving the RED (C3), the high pressure fluidizing gas is thus recovered by the expander (GT1) for electricity generation. The reactions in the RED assumed to occur during reduction are as follows [37]:

$$Fe_2O_3 + CO \rightarrow 2FeO + CO_2 \qquad \Delta H = -2.8 \text{ kJ mol}^{-1} \tag{2}$$

$$FeO + CO \rightarrow Fe + CO_2 \qquad \Delta H = -11 \text{ kJ mol}^{-1} \tag{3}$$

$$Fe_2O_3 + H_2 \rightarrow 2FeO + H_2O \qquad \Delta H = 38.4 \text{ kJ mol}^{-1} \tag{4}$$

$$FeO + H_2 \rightarrow Fe + H_2O \qquad \Delta H = 30.2 \text{ kJ mol}^{-1} \tag{5}$$

$$4Fe_2O_3 + 3CH_4 \rightarrow 8Fe + 3CO_2 + 6H_2O \qquad \Delta H = 897.18 \text{ kJ mol}^{-1} \tag{6}$$

The formation of by-products, including Fe_3C and carbon soot due to Boudouard reaction has been noticed in the continuous operation in RED. However, efforts to diminish the formation of Fe_3C have been performed in previous studies, including the modification of iron-based oxygen carrier with CeO_2 and exhaustive selection of the used iron-based oxygen carriers [38].

CO_2 and steam are generated during the reduction step and then leave the reducer for the cooling process in preparation for separation (CD1). The separated CO_2 (C7) is then compressed and ready for the sequestration purposes. Other product from the reduction step, the

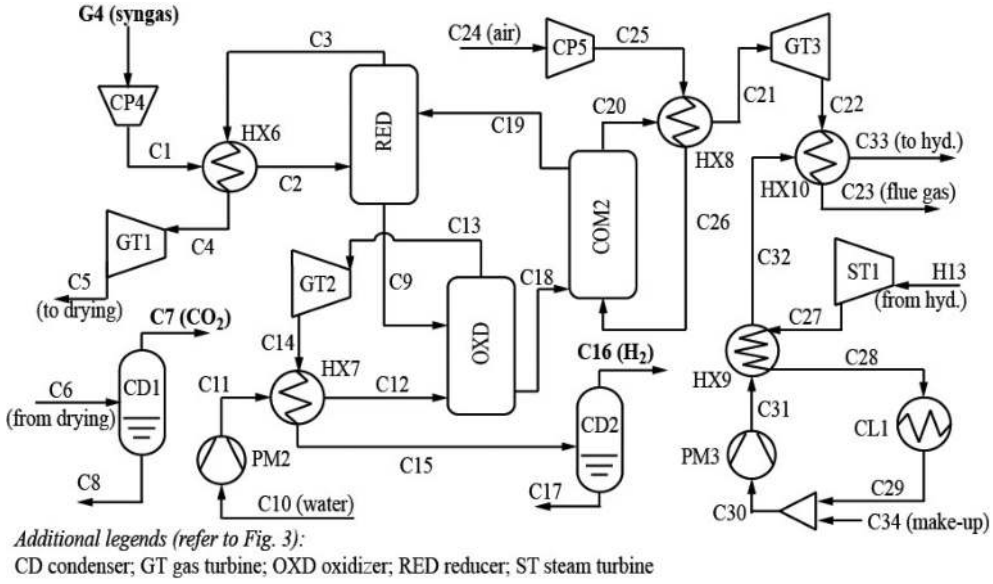

Figure 4. Process flow diagram of the chemical looping and combined cycle modules.

iron particles (C9), is fed to the OXD in which the oxidation takes place with the steam as reactant to produce highly pure H_2 (C16). The reactions inside the OXD in the presence of excess steam can be written as follows:

$$Fe + H_2O \rightarrow FeO + H_2 \qquad \Delta H = -30.2 \text{ kJ mol}^{-1} \tag{7}$$

$$3FeO + H_2O \rightarrow Fe_3O_4 + H_2 \qquad \Delta H = -60.6 \text{ kJ mol}^{-1} \tag{8}$$

The generated H_2 is discharged to the hydrogenation module for further process, while the metals move to the COM2 for recirculation. The reaction inside the COM2 is shown below.

$$4Fe_3O_4 + O_2 \rightarrow 6Fe_2O_3 \qquad \Delta H = -471.6 \text{ kJ mol}^{-1} \tag{9}$$

The reduction process is performed by the discharged heat from the combustion process implanted inside the metal oxide. The high energy from compressed flue gas is expanded for electricity generation in GT3 and ST1 by employing combined cycle. The conditions of chemical looping and combined cycle modules are explained in **Table 3**.

3.1.3.3. Hydrogenation

The conditions during toluene hydrogenation and the schematic flow diagram are shown in **Table 4** and **Figure 5**, respectively. The heat generated from the exothermic reaction of hydrogenation is applied as the heat source for electricity generation in the steam turbine (ST1). The theoretical gravimetric and volumetric hydrogen concentrations in MCH under ambient conditions are 6.2 and 47%, respectively [39]. The hydrogenation reaction is as follows:

$$C_7H_8 + 3H_2 \rightarrow C_7H_{14} \qquad \Delta H = -205.0 \text{ kJ mol}^{-1} \tag{10}$$

3.1.4. Performance of integrated system

Figure 6 indicates the effect of drying fluidization velocities to the compressor and blower duties, net generated power, and power efficiency. These values are carried out using a steam-to-fuel ratio during gasification and a basic chemical looping pressure of 0.9 and 3 MPa, respectively. A compressor (CP4) is prepared after the gasification module to pressurize the syngas into the pressure of chemical looping.

Based on the calculation results, there is barely significant shift in the compressor duty as the compression work is almost constant at 1.8 MW. On the other hand, the duty of blower is increasing as the fluidization velocities during drying are uprising. Here, the blower duty at the lowest fluidization velocity ($U_{mf,dry}$, 1.28 m s^{-1}) is 0.7 MW and rise to 2.7 MW when the fluidization velocity is increased to 4 $U_{mf,dry}$. As high amount of energy is required for the high duty of the blower, a rapid fluidization velocity during drying results in a lower total efficiency.

Figure 7(a) presents the effect of different steam-to-fuel ratios to the amount of H_2 generated, H_2 production efficiency, net generated power, and the total efficiency, while **Figure 7(b)** presents the effect of different steam-to-fuel ratios to the amounts of produced H_2 and MCH. These values are carried out using a specific fluidization velocity during drying and a basic

Component	Value	Note
Reducer		
Temperature (K)	1073	
Pressure (MPa)	2.0–4.0	
Syngas conversion (%)	100	
Iron particle diameter (mm)	2	
Produced CO_2 purity (%)	99.99	
Oxidizer		
Temperature (K)	1023	
Pressure (MPa)	2.0–4.0	
Produced H_2 purity (%)	99.99	
Excess steam at outlet (%)	10	
Combustor		
Temperature (K)	1473	
Pressure (MPa)	2.2–4.2	
Air excess at outlet (%)	10	
Gas turbine (F-class)		
Turbine polytrophic efficiency (%)	90	
Maximum turbine inlet temperature (K)	1473	
HRSG and steam turbine		
Turbine polytrophic efficiency (%)	90	
Inlet pressure (MPa)	15	
Maximum turbine inlet temperature (K)	973	
Minimum outlet vapor quality	0.9	

Table 3. Conditions and assumptions for chemical looping and the combined cycle.

Component	Value
Reaction temperature (K)	473
Operating pressure (kPa)	130
Catalyst	Ni-Mo/Al_2O_3
Catalyst particle size (mm)	0.3
Particle sphericity	0.5

Table 4. Conditions assumed for toluene hydrogenation.

chemical looping pressure of 2 $U_{mf,dry}$ and 3 MPa, respectively. Generally, the higher H_2 production efficiency and power generation are both achieved in the steam-to-fuel ratio of 0.9 instead of 1.4. The produced H_2 amount and net generated power at a steam-to-fuel ratio of 1.4 are 4.3 t h^{-1} (H_2 production efficiency of 66.5%) and 24.1 MW (power generation efficiency of 11.2%), respectively. These values rise up to 4.6 t h^{-1} (with a H_2 production efficiency of 71.9%) and 26.3 MW (with a power generation efficiency of 12.2%), when the steam-to-fuel ratio is set at 0.9.

Figure 8 Shows the effect of basic chemical looping pressure to the net generated power and power generation efficiency. These values are carried out by applying a fluidization velocity during drying and a steam-to-fuel ratio during gasification of 2 $U_{mf,dry}$ and 0.9, respectively.

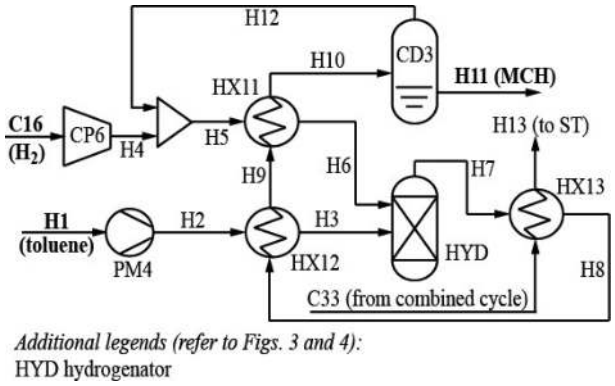

Figure 5. Process flow diagram of the hydrogenation module.

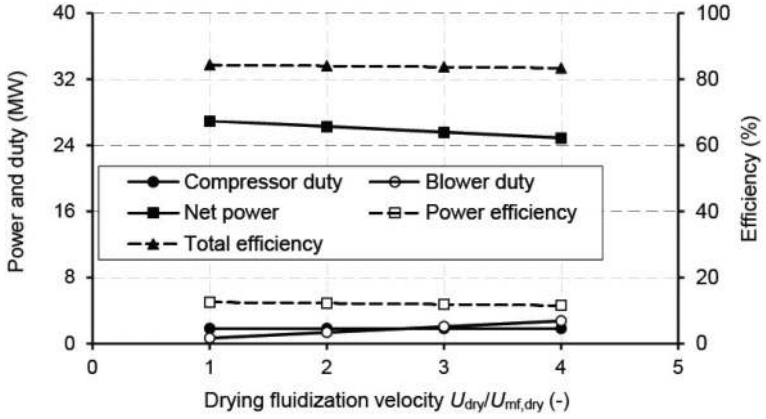

Figure 6. Effect of fluidization velocity during drying (at a steam-to-fuel ratio during gasification and basic chemical looping pressure of 0.9 and 3 MPa, respectively).

Generally, the increase of chemical looping process pressures leads to increase in both the net generated power and the power generation efficiency.

3.2. Integrated systems from microalgae by supercritical water gasification

3.2.1. The characteristics of microalgae as energy source

Besides the high potential in the pharmaceuticals, industrial materials, and food production, microalgae own a high potential for the energy source [40]. Among other biomasses, microalgae are very exceptional due to its excellent growth rate, ability to grow in a harsh environment, and highly efficient solar energy conversion [4]. Currently, many products of fuel are derived from the microalgae, including bio-oil, biohydrogen, and biodiesel [41]. However, as the microalgae grow in an aqueous environment far from the industrial or residential area, it has to be planted remotely and transported to the designated area for the utilization of microalgae

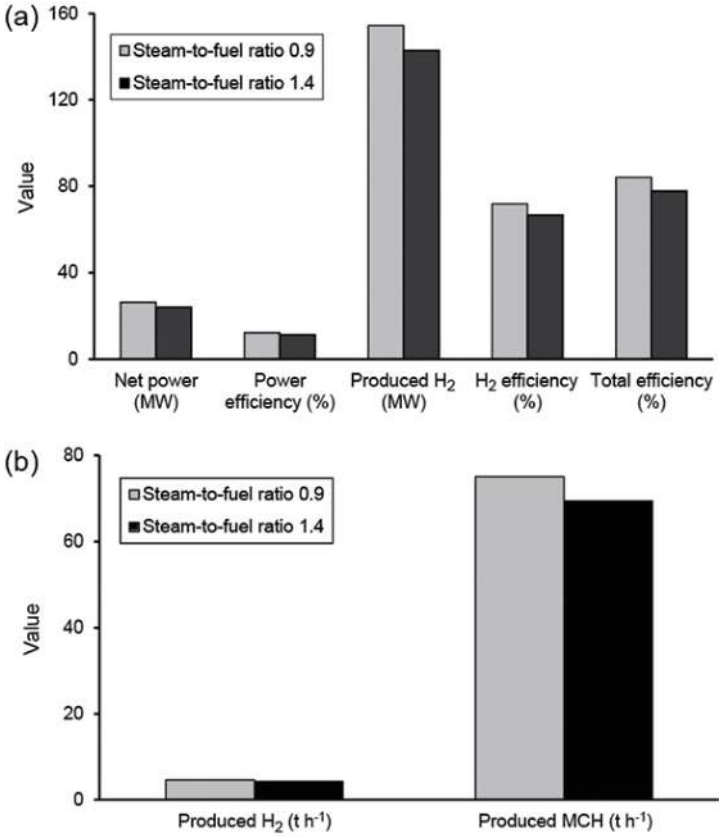

Figure 7. Effects of the steam-to-fuel ratio on (a) net generated power, power generation efficiency, produced H_2, H_2 production efficiency, and total efficiency and (b) produced H_2 and MCH amounts (U_{dry} = 2 $U_{mf,dry}$, basic chemical looping pressure = 3 MPa).

in the large scale. To this, a process chain from the microalgae cultivation to the H_2-based MCH for LOHC generation can solve the transportation and storage issues of the large-scale utilization of microalgae.

For the investigation, an alga species with ability to grow rapidly in normal condition and rich protein is necessary. To this, *Chlorella vulgaris* is selected as a sample for system evaluation. [42]. The properties of *Chlorella vulgaris*, including the results of proximate and ultimate analyses are listed in **Table 5**.

Among any candidates in the thermochemical process, gasification owns the highest rank due to its conversion efficiency [43]. There are two gasification methods widely used, the conventional thermal gasification and supercritical water gasification (SCWG). The former requires drying process to low moisture content before the gasification, while the latter is performed in the aqueous state, in which drying process is avoidable [44], and more favorable for the gasification of microalgae, owing to its high moisture content (70–90 wt% wb) [16]. However, SCWG is an energy

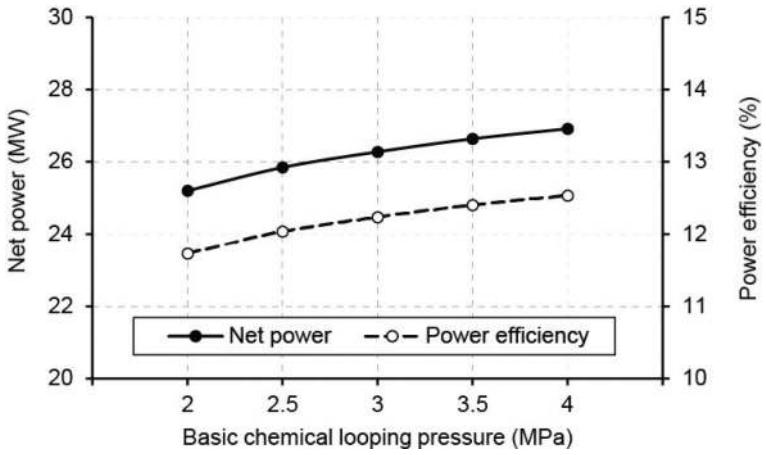

Figure 8. Correlations of net generated power and power generation efficiency with basic chemical looping pressure (U_{dry} = 2 $U_{mf,dry}$, steam-to-fuel ratio = 0.9).

Property	Value
Moisture content (wt% wb)	90
Dry solid content (wt% wb)	10
Chemical composition	
Protein (wt% db)	64.1
Fat (wt% db)	13
Fiber (wt% db)	21.1
Ash (wt% db)	7
Carbohydrates (wt% db)	15
Ultimate analysis	
Carbon (wt% db)	45.8
Hydrogen (wt% db)	7.9
Nitrogen (wt% db)	7.5
Oxygen (wt% db)	38.7
Calorific value (dried, MJ kg^{-1})	18.49

Table 5. Proximate and ultimate analyses of *Chlorella vulgaris*.

consuming process, which tends to absorb a huge portion of energy and create a lowly energy-efficient system [45]. To this, the EPI technology can tackle the challenge of the high energy issue of the SCWG, and leads to a novel process for the large-scale utilization of microalgae into LOHC.

3.2.2. Integrated system development

The basic schematic energy and material flows of the integrated system consists of SCWG, H_2 separation, hydrogenation, and the combined cycle. **Figure 9** explains the detailed schematic process flow diagram of the proposed integrated system.

3.2.3. Analysis of integrated system

3.2.3.1. Supercritical water gasification of microalgae

Due to the supercritical regime of the reaction, the decreasing water density causes a low static relative dielectric constant, hence, weaken the hydrogen bonds and improve the yield of the syngas [13]. Moreover, syngas cleaning can be disregarded due to no formation of NO_x or SO_x in the process. In the proposed process, a fluidized-bed reactor was selected due to its beneficial characteristics, including better particle mixing, ability to avoid plugging, uniform temperature distribution, and a high conversion rate [46].

For high performance of gasification, a catalyst set of Ru/TiO_2 which exhibits H_2-rich syngas and complete carbon conversion is injected inside the gasifier. Moreover, fluidizing particles (e.g., alumina) can be proposed to increase the particle dynamics inside the reactor and prevent the production of ash layer and char on the reactor wall [47]. In this study, the flow rate and initial moisture content of wet microalgae are fixed at 1000 t h^{-1} and 90 wt% wb, respectively. Two gasification pressures are evaluated: 25 and 30 MPa. **Table 6** gives the gasification conditions and produced syngas composition.

3.2.3.2. H_2 Separation and hydrogenation

Membrane-based separation is adopted for the H_2 extraction from the syngas. This method promotes low energy consumption, simple handling process, and mild conditionings. Among the membrane separation methods, polymeric membrane separation, consists of microporous film acting as a semipermeable barrier, owns the widest commercial application [48]. The assumed conditions during H_2 separation and hydrogenation are given in **Table 7**.

Property	Value
SCWG condition	
Temperature (°C)	600
Pressure (MPa)	25, 30
Fluidization velocity U/U_{mf} (−)	1, 2, 3, 4
Fluidizing material (−)	alumina
Density (kg m^{-3})	3400
Particle diameter (mm)	0.3
Sphericity (−)	0.67
Voidage at minimum fluidization (−)	0.45
Gasification catalyst (−)	Ru/TiO_2
Weight ratio of catalyst to wet algae (−)	2
Syngas composition	
Carbon conversion efficiency (%)	100
H_2 (dry mol%)	46.1
CO (dry mol%)	3.1
CH_4 (dry mol%)	18.1
C_2H_6 and C_3H_8 (dry mol%)	4.9
CO_2 (dry mol%)	27.8

Table 6. SCWG conditions and syngas composition used during calculation.

Property	Value
Separation	
Type (−)	Polymeric membrane
Hydrogen recovery (%)	70
Operating temperature (°C)	100
Feed inlet pressure (kPa)	800
Product outlet pressure (kPa)	110.0
Product H_2 concentration (mol%)	0.995
Product CO concentration (mol%)	0.000498
Product other gas concentration (mol%)	0.00448
Hydrogenation	
Pressure (kPa)	130
Temperature (°C)	200
Catalyst (−)	Ni-Mo/Al_2O_3
Catalyst particle size (mm)	0.3
Sphericity (−)	0.5

Table 7. Hydrogen separation and hydrogenation conditions.

3.2.3.3. Combined cycle and power generation

After the H_2 is separated from the syngas, the remaining syngas is employed as a fuel for combustion (COMB) in the combined cycle. Moreover, due to high temperature of the flue gas from the gas turbine (GT), it is thus used to superheat the mixture of syngas and steam from the SCWG reactor. At last, the remaining heat is recovered in HRSG for the steam turbine (ST). The conditions of the combined cycle modules, including combustor, gas and steam turbines are presented in **Table 8**.

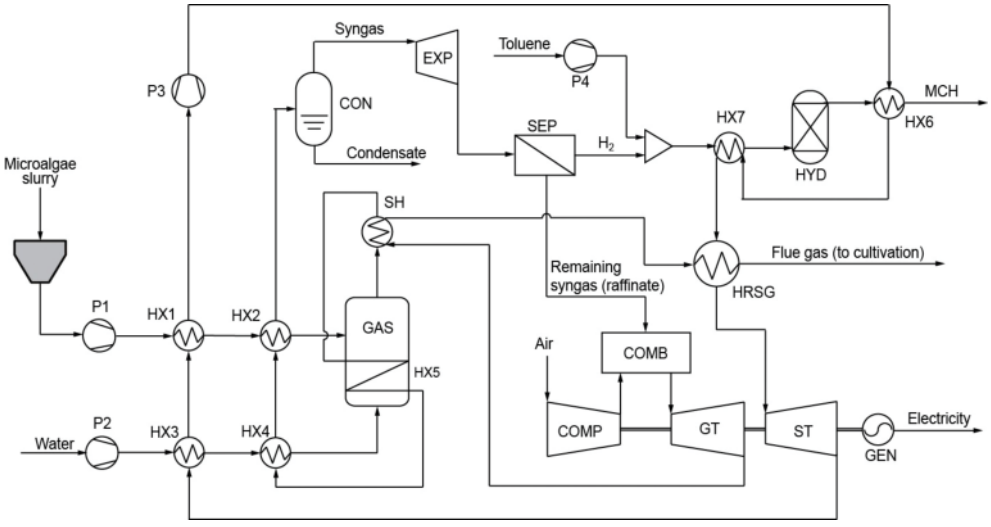

Figure 9. Schematic diagram of the process flow of the proposed integrated system.

3.2.4. Performance of integrated system

Figure 10 shows the relationship between total energy efficiency, η_{tot}, and fluidization velocity for different gasification pressures of 25 and 30 MPa. Subsequently, about 3.5 t-H_2 h^{-1} can be converted to MCH by hydrogenation process with toluene. The increase of fluidization velocity leads to lower total energy efficiency. Therefore, gasification carried out under a lower gasification pressure at 25 MPa has better total energy efficiency than that at 30 MPa.

The increasing in fluidization velocity leads to more water for the fluidizing steam which thus increases the flow rate of steam exhausted from the SCWG reactor. As a result, the heat available as hot stream in the HRSG decreases, leading to a decrease in actual work obtained from the steam turbine. On the other hand, the increasing of gasification pressure leads to more flow rate of the fluidizing steam under same fluidization velocity. Thus, the increase in gasification pressure finally leads to lower actual work by the steam turbine.

Property	Value
Combustor and gas turbine	
Compressor outlet pressure (MPa)	2
Compressor polytrophic efficiency (%)	87
Combustor pressure drop (%)	2
Gas turbine inlet temperature (°C)	1300
Gas turbine adiabatic efficiency (%)	90
Air to fuel ratio (−)	10
HRSG and steam turbine	
HRSG outlet pressure (MPa)	10
Heat exchanger temperature difference (°C)	10
HRSG pressure drop (%)	1
Steam turbine inlet temperature (°C)	600
Steam turbine polytrophic efficiency (%)	90
Minimum outlet vapor quality (%)	90

Table 8. Assumed conditions for the combined cycle, including combustion and gas and steam turbines.

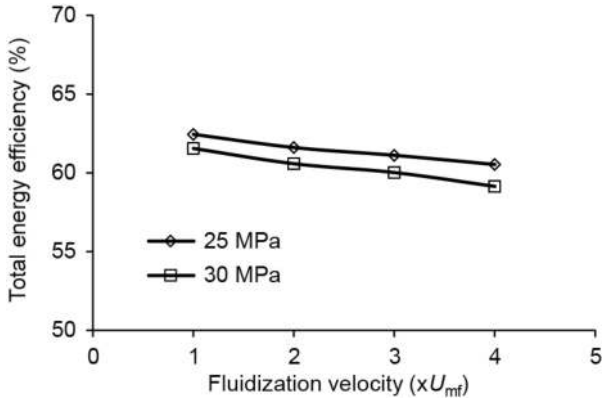

Figure 10. Relationship between total energy efficiency and fluidization velocity under different gasification pressures.

4. Conclusion

Novel integrated gasification systems for coproduction of electricity and MCH from low-rank coal and microalgae have been proposed. Enhanced process integration technology is applied for both systems to minimize exergy losses throughout the integrated system, thus improving the total energy efficiency. However, the models are carried out in the condition of ideal zero heat loss. Therefore, approximately 5–10% of heat losses are necessary to consider for the investigation in the actual case of the systems. For the case of microalgae, the effects of the fluidization velocity and gasification pressure on the total energy and electricity generation efficiencies were evaluated for optimum integrated system, while for the case of low-rank coal, the optimization is subjected to the investigation of fluidization velocity, steam-to-fuel ratio, and the chemical looping pressure. Finally, the integrated system for microalgae is capable to provide more than 60% of total energy efficiency, while the integrated system for low-rank coal delivers the total energy efficiency of 84%.

Author details

Lukman Adi Prananto and Muhammad Aziz*

*Address all correspondence to: maziz@ssr.titech.ac.jp

Institute of Innovative Research, Tokyo Institute of Technology, Japan

References

[1] Bilgen S. Structure and environmental impact of global energy consumption. Renewable & Sustainable Energy Reviews. 2014;**38**:890-902

[2] Aziz M, Zaini IN, Oda T, Morihara A, Kashiwagi T. Energy conservative brown coal conversion to hydrogen and power based on enhanced process integration: Integrated drying, coal direct chemical looping, combined cycle and hydrogenation. International Journal of Hydrogen Energy. 2017;**42**(5):2904-2913

[3] Aziz M. Power generation from algae employing enhanced process integration technology. Chemical Engineering Research and Design. 2016;**109**:297-306

[4] Aziz M, Oda T, Kashiwagi T. Advanced energy harvesting from macroalgae-innovative integration of drying, gasification and combined cycle. Energies. 2014;**7**(12):8217-8235

[5] Darmawan A, Budianto D, Aziz M, Tokimatsu K. Retrofitting existing coal power plants through cofiring with hydrothermally treated empty fruit bunch and a novel integrated system. Applied Energy. 2017;**204**:1138-1147

[6] Yavor Y, Goroshin S, Bergthorson JM, Frost DL. Comparative reactivity of industrial metal powders with water for hydrogen production. International Journal of Hydrogen Energy. 2015;**40**(2):1026-1036

[7] Miura D, Tezuka T. A comparative study of ammonia energy systems as a future energy carrier, with particular reference to vehicle use in Japan. Energy. 2014;**68**:428-436

[8] Aziz M. Integrated hydrogen production and power generation from microalgae. International Journal of Hydrogen Energy. 2016;**41**(1):104-112

[9] Teichmann D, Arlt W, Wasserscheid P. Liquid organic hydrogen carriers as an efficient vector for the transport and storage of renewable energy. International Journal of Hydrogen Energy. 2012;**37**(23):18118-18132

[10] Aziz M, Oda T, Kashiwagi T. Clean hydrogen production from low rank coal: Novel integration of drying, gasification, chemical looping, and hydrogenation. Chemical Engineering Transactions. 2015;**45**:613-618

[11] Müller K, Aslam R, Fischer A, Stark K, Wasserscheid P, Arlt W. Experimental assessment of the degree of hydrogen loading for the dibenzyl toluene based LOHC system. International Journal of Hydrogen Energy. 2016;**41**(47):22097-22103

[12] Okada Y, Shimura M. Development of large-scale H_2 storage and transportation technology with liquid organic hydrogen carrier (LOHC). In: The 21st joint GCC-Japan environment symposium; 5–6 February 2015; Doha, Qatar: 2013. pp. 5793-5803

[13] Aziz M. Integrated supercritical water gasification and a combined cycle for microalgal utilization. Energy Conversion and Management. 2015;**91**:140-148

[14] Zaini IN, Nurdiawati A, Aziz M. Cogeneration of power and H_2 by steam gasification and syngas chemical looping of macroalgae. Applied Energy. 2017;**207**:134-145

[15] Aziz M, Juangsa FB, Kurniawan W, Budiman BA. Clean co-production of H_2 and power from low rank coal. Energy. 2016;**116**:489-497

[16] Aziz M, Oda T, Kashiwagi T. Integration of energy-efficient drying in microalgae utilization based on enhanced process integration. Energy. 2014;**70**:307-316

[17] Aziz M, Kansha Y, Tsutsumi A. Self-heat recuperative fluidized bed drying of brown coal. Chemical Engineering and Processing: Process Intensification. 2011;**50**(9):944-951

[18] Aziz M, Kansha Y, Kishimoto A, Kotani Y, Liu Y, Tsutsumi A. Advanced energy saving in low rank coal drying based on self-heat recuperation technology. Fuel Processing Technology. 2012;**104**:16-22

[19] Prabowo B, Aziz M, Umeki K, Susanto H, Yan M, Yoshikawa K. CO_2-recycling biomass gasification system for highly efficient and carbon-negative power generation. Applied Energy. 2015;**158**:97-106

[20] Aziz M, Kurniawan T, Oda T, Kashiwagi T. Advanced power generation using biomass wastes from palm oil mills. Applied Thermal Engineering. 2017;**114**:1378-1386

[21] Darmawan A, Hardi F, Yoshikawa K, Aziz M, Tokimatsu K. Enhanced process integration of black liquor evaporation, gasification, and combined cycle. Applied Energy. DOI: 10.1016/j.apenergy.2017.05.058

[22] Dincer I, Acar C. Review and evaluation of hydrogen production methods for better sustainability. International Journal of Hydrogen Energy. 2014;**40**(34):11094-11111

[23] Aziz M, Budianto D, Oda T. Computational fluid dynamic analysis of co-firing of palm kernel shell and coal. Energies. 2016;**9**(3):137

[24] Yamaguchi D, Sanderson PJ, Lim S, Aye L. Supercritical water gasification of Victorian brown coal: Experimental characterisation. International Journal of Hydrogen Energy. 2009;**34**:3342-3350

[25] Zhang Y, Jin B, Zou X, Zhao H. A clean coal utilization technology based on coal pyrolysis and chemical looping with oxygen uncoupling: Principle and experimental validation. Energy. 2016;**98**:181-189

[26] Li P, Pan SY, Pei S, Lin YJ, Chiang PC. Challenges and perspectives on carbon fixation and utilization technologies: An overview. Aerosol and Air Quality Research. 2016;**16**(6):1327-1344

[27] Minutillo M, Perna A. Renewable energy storage system via coal hydrogasification with co-production of electricity and synthetic natural gas. International Journal of Hydrogen Energy. 2014;**39**(11):5793-5803

[28] Xiang W, Chen S, Xue Z, Sun X. Investigation of coal gasification hydrogen and electricity co-production plant with three-reactors chemical looping process. International Journal of Hydrogen Energy. 2010;**35**(16):8580-8591

[29] Cleeton JPE, Bohn CD, Müller CR, Dennis JS, Scott SA. Clean hydrogen production and electricity from coal via chemical looping: Identifying a suitable operating regime. International Journal of Hydrogen Energy. 2009;**34**(1):1-12

[30] Chen Z, Agarwal PK, Agnew JB. Steam drying of coal. Part 2. Modeling the operation of a fluidized bed drying unit. Fuel. 2001;**80**(2):209-223

[31] Xianchun L, Hui S, Qi W, Meesri C, Terry WALL, Jianglong Y. Experimental study on drying and moisture re-adsorption kinetics of an Indonesian low rank coal. Journal of Environmental Sciences. 2009;**21**:S127-S130

[32] Pawlak-Kruczek H, Plutecki Z, Michalski M. Brown coal drying in a fluidized bed applying a low-temperature gaseous medium. Drying Technology. 2014;**32**(11):1334-1342

[33] Cormos CC, Starr F, Tzimas E, Peteves S. Innovative concepts for hydrogen production processes based on coal gasification with CO_2 capture. International Journal of Hydrogen Energy. 2008;**33**(4):1286-1294

[34] Ruiz JA, Juárez MC, Morales MP, Muñoz P, Mendívil MA. Biomass gasification for electricity generation: Review of current technology barriers. Renewable and Sustainable Energy Reviews. 2013;**18**:174-183

[35] Gnanapragasam NV, Reddy BV, Rosen MA. Hydrogen production from coal using coal direct chemical looping and syngas chemical looping combustion systems: Assessment of system operation and resource requirements. International Journal of Hydrogen Energy. 2009;**34**(6):2606-2615

[36] Tong A, Sridhar D, Sun Z, Kim HR, Zeng L, Wang F, Wang D, Kathe MV, Luo S, Sun Y, Fan LS. Continuous high purity hydrogen generation from a syngas chemical looping 25 kWth sub-pilot unit with 100% carbon capture. Fuel. 2013;**103**:495-505

[37] Fan LS. Chemical Looping Systems for Fossil Energy Conversions. John Wiley & Sons; 2011

[38] Sun S, Zhao M, Cai L, Zhang S, Zeng D, Xiao R. Performance of CeO_2-modified iron-based oxygen carrier in the chemical looping hydrogen generation process. Energy and Fuels. 2015;**29**(11):7612-7621

[39] Biniwale RB, Rayalu S, Devotta S, Ichikawa M. Chemical hydrides: A solution to high capacity hydrogen storage and supply. International Journal of Hydrogen Energy. 2008; **33**(1):360-365

[40] Wang B, Li Y, Wu N, Lan CQ. CO_2 bio-mitigation using microalgae. Applied Microbiology and Biotechnology. 2008;**79**(5):707-718

[41] Aziz M, Oda T, Kashiwagi T. Enhanced high energy efficient steam drying of algae. Applied Energy. 2013;**109**:163-170

[42] Cersosimo M, Brunetti A, Drioli E, Fiorino F, Dong G, Woo KT, Lee J, Lee YM, Barbieri G. Separation of CO_2 from humidified ternary gas mixtures using thermally rearranged polymeric membranes. Journal of Membrane Science. 2015;**492**:257-262

[43] Aziz M, Prawisudha P, Prabowo B, Budiman BA. Integration of energy-efficient empty fruit bunch drying with gasification/combined cycle systems. Applied Energy. 2015;**139**: 188-195

[44] Lu Y, Jin H, Guo L, Zhang X, Cao C, Guo X. Hydrogen production by biomass gasification in supercritical water with a fluidized bed reactor. International Journal of Hydrogen Energy. 2008;**33**(21):6066-6075

[45] Fiori L, Valbusa M, Castello D. Supercritical water gasification of biomass for H_2 production: Process design. Bioresource Technology. 2012;**121**:139-147

[46] Matsumura Y, Minowa T. Fundamental design of a continuous biomass gasification process using a supercritical water fluidized bed. International Journal of Hydrogen Energy. 2004;**29**(7):701-707

[47] Chakinala AG, Brilman DWF, Van Swaaij WPM, Kersten SRA. Catalytic and non-catalytic supercritical water gasification of microalgae and glycerol. Industrial and Engineering Chemistry. 2010;**49**(3):1113-1122

[48] Liu K, Song C, Subramani V. Hydrogen and Syngas Production and Purification Technologies. John Wiley & Sons. 2009